Molecular and Mesoscopic Structures of Transparent Block Copolymer−Silica Monoliths

N. A. Melosh,[†,§] P. Lipic,[‡] F. S. Bates,[‡] F. Wudl,[#,§,⊥] G. D. Stucky,[#,§] G. H. Fredrickson,[†,§] and B. F. Chmelka*[,†]

Departments of Chemical Engineering, Chemistry, and Materials, University of California, Santa Barbara, California 93106, and Department of Chemical Engineering and Materials Science, University of Minnesota, Minneapolis, Minnesota 55455

Received November 6, 1998

ABSTRACT: Mesoscopically ordered, transparent silica−surfactant monoliths have been prepared using amphiphilic triblock poly(ethylene oxide)−poly(propylene oxide)−poly(ethylene oxide) (PEO−PPO−PEO) copolymer species to organize polymerizing silica networks. The block copolymer acts as a structure-directing agent, as the aqueous silica cations partition within the hydrophilic regions of the self-assembled system and associate preferentially with the PEO blocks. Subsequent polymerization of the silica precursor species under strongly acidic conditions (pH ∼1) produces a densely cross-linked silica network that may be mesoscopically organized by the block copolymer species into composites with characteristic ordering length scales of >10 nm. When this is accompanied by slow evaporation of the aqueous solvent, such composite mesostructures can be formed into transparent and crack-free monoliths (e.g., 2.5 cm diameter × 3 mm thick). Distributions and dynamics of the PEO and PPO copolymer blocks within the silica matrix were investigated in situ using $^{29}Si\{^1H\}$ and $^{13}C\{^1H\}$ two-dimensional solid-state heteronuclear correlation NMR techniques and ^1H NMR relaxation measurements. Mesostructural ordering was determined by X-ray diffraction and transmission electron microscopy. The degree of microphase separation and the resulting mesostructure of bulk samples were found to depend strongly upon the concentration of block copolymer, with higher concentrations producing higher degrees of order.

Introduction

Over the past few years, a great deal of interest has developed in using hydrophilic−hydrophobic surfactants or block copolymers to organize polymerizable species under conditions where hydrophilic components form continuous regions within a mesostructurally ordered system. Noteworthy examples are the M41S family of materials and analogues, in which polymerizable metal oxide species are selectively incorporated into aqueous domains located between low-molecular-weight surfactant aggregates.[1−3] Mesoscopic order is imparted by typically cooperative self-assembly of the inorganic and surfactant species interacting across their hydrophilic−hydrophobic interfaces.[4] The inorganic species are then cross-linked to form dense, continuous metal oxide networks. The resulting mesostructurally ordered inorganic−organic composite materials have been produced in the form of powders,[1,5,6] films,[7−9] or opaque monoliths,[10,11] which have generally seen limited utility for optical applications. Several groups have advanced the processability of such low-molecular-weight surfactant-based organic/inorganic systems.[12−14] For example, Ryoo et al.[12] have prepared transparent mesoscopically ordered thick films, and Marlow et al.[14] have reported laser and waveguide properties for fiberlike particles of mesoscopically ordered silica doped with rhodamine dye species.

Recently, we and others have developed synthesis strategies that use amphiphilic block copolymers as structure-directing agents to produce mesoscopically ordered inorganic−organic composites with large characteristic length scales (up to 30 nm) and improved processability.[15−17] Such approaches are analogous to recent preparations of a closely related, but wholly organic, system, in which hydrophilic−hydrophobic block copolymer species were used to organize a polymerizable epoxy resin.[18] An important benefit of using block copolymers as structure-directing agents for inorganic oxide networks is the attractive processing advantages that these species present. By adjusting the composition, architecture, and molecular weight of the block copolymer species, the phase, ordering length scale (∼5−40 nm), and macroscopic morphologies of the self-assembled structures can be controlled. Furthermore, these materials can be processed to obtain high degrees of both mesoscopic organization and macroscopic transparency, for instance in fibers[19] and thin films.[9] The two together open the possibility of incorporating substantially higher concentrations of organic guest molecules into thermally stable transparent composites, which are often limited by their solubilities in non-mesostructured sol−gel-derived inorganic matrices. Göltner et al. have recently demonstrated that transparent inorganic−organic monoliths with wormlike aggregate mesostructures can be prepared, though the resulting composites cracked upon exposure to dry air.[20] Optical uses for such materials have, as a consequence, remained largely unrealized.

We report here the synthesis and characterization of highly ordered, transparent and crack-free silica/block copolymer monoliths based upon block copolymer structure-directing agents. This has been achieved by selectively incorporating and cross-linking hydrolyzed silica precursor species into the aqueous regions of a concentrated amphiphilic poly(ethylene oxide)−poly(propylene

[†] Department of Chemical Engineering, UC, Santa Barbara.
[#] Department of Chemistry, UC, Santa Barbara.
[§] Materials Department, UC, Santa Barbara.
[‡] University of Minnesota.
[⊥] Present address: Department of Chemistry and Biochemistry, University of California, Los Angeles, CA 90095.
* To whom correspondence should be addressed.

10.1021/ma9817323 CCC: $18.00
Published on Web 06/11/1999

oxide)−poly(ethylene oxide) (PEO−PPO−PEO) block copolymer mesophase. The structures and dynamics of the PEO−PPO−PEO block copolymer and silica components were investigated using solid-state NMR, together with XRD and TEM analyses, to correlate molecular, mesoscopic, and macroscopic material properties.

Experimental Section

The transparent monolithic block copolymer/silica composites were prepared by dissolving amphiphilic PEO−PPO−PEO species in an acidic ethanol/water solution (ca. pH 1.5), swelling the hydrophilic PEO block with soluble aqueous silica ions, and subsequently polymerizing the silica species to form a rigid silica network. This study has focused on the use of $(\text{ethylene oxide})_{106}(\text{propylene oxide})_{70}(\text{ethylene oxide})_{106}$ (EO_{106}-$PO_{70}EO_{106}$, Pluronic F127) as the structure-directing amphiphilic species. At concentrations greater than 20 wt % in water, this system possesses structures of cubic-packed arrays of spherical aggregates. Bicontinuous cubic, hexagonal, or lamellar mesophases can be produced by adding a small amount of a hydrophobic swelling agent, such as butanol or xylene.[21] In the presence of a silica sol under strongly acidic conditions, the hydrophilic PEO blocks associate with hydrolyzed silica cations via complexation interactions.[22] As a consequence, the silica species adopt the mesoscopic organization imposed by the block copolymer species, partitioning preferentially into the hydrophilic regions of the sample, where they form a rigid cross-linked network. The process can be catalyzed by either acids or bases; however, under the conditions used here, the acidic catalyst was found to form better monoliths. The details of similar sol−gel processing without the presence of structure-directing agents have been treated elsewhere.[23,24]

The transparent block copolymer/silica monoliths were prepared specifically as follows: a calculated amount of a 20 wt % Pluronic F127/ethanol (EtOH) solution was measured into a 30 mL vial, followed by 0.72 mL of aqueous HCl (pH 1.4), and stirred until the block copolymer had completely dissolved. The F127 was used as received from BASF USA (Mount Olive, NJ). While still stirring, 1.0 mL of tetraethoxysilane (TEOS, Aldrich Chemicals) was added, forming a homogeneous mixture in approximately 10 min. The molar ratio of H_2O to TEOS was held constant at 9:1 to ensure complete hydrolysis of the TEOS, as well as to provide the water necessary for the formation of the desired phase with the block copolymer. After gelation (1−2 days) uncovered under ambient conditions, the sample vials were sealed for 2 weeks and held at room temperature. At the end of this period, the dried products had shrunk from 0 to 50% in diameter, depending on the concentration of block copolymer present, while the thicknesses decreased slightly. All of the dried composites retained the shape of their respective containers. The samples were subsequently uncovered and stored at room temperature to allow excess solvent to evaporate. The composites formed 2−3 mm thick, 1.5−2.5 cm diameter transparent disks, an example of which is shown in Figure 1. Table 1 presents synthesis and characterization parameters for a series of Pluronic F127/silica composites that were systematically prepared with compositions from 0 to 62 wt % F127 copolymer. Under these processing conditions, samples with 70 wt % polymer or above formed opaque composites that are undesirable for optical device applications. An identical series of composites was produced with ^{2}HCl, $C_2H_5O^2H$, and ^2H_2O to eliminate ^{1}H NMR signals from surface silanol groups. X-ray scattering analyses of these materials showed similar diffraction patterns as obtained for the fully protonated composites.

Small-angle powder X-ray diffraction (XRD) patterns were collected on a Pad-X Scintag X-ray diffractometer using Cu Kα radiation with scattering reflections measured over 2θ angles between 0.2° and 4.0°, corresponding to d spacings between 44 and 2.2 nm. Scans were collected at 0.01° increments with 5 s averaging per point at room temperature. Strong attenuation of the X-ray beam by the bulk monolithic samples required that they be analyzed after being gently ground into powders. Equivalent volumes were used for each sample to allow approximate quantitative comparisons of the XRD scattering intensities.

Figure 1. A mesostructurally ordered transparent block copolymer/silica monolith, prepared with a composition of 62 wt % $EO_{106}-PO_{70}-EO_{106}$. The monolithic disk is 2.5 cm in diameter and 3 mm thick.

TEM samples were prepared by embedding powders from ground monoliths into epoxy matrices, which were cut into 100 nm sections with a Leica UltraCut R ultramicrotome. The sections were then transferred onto 400 mesh Cu grids and examined with a JEOL JEM 1210 transmission electron microscope operating at 125 keV.

NMR Experiments. All solid-state ^{1}H, ^{13}C, and ^{29}Si NMR experiments were performed on a Chemagnetics CMX-500 spectrometer operating at frequencies of 498.616 MHz for ^{1}H, 125.382 MHz for ^{13}C, and 99.060 MHz for ^{29}Si. ^{1}H, ^{13}C, and ^{29}Si chemical shifts have been referenced to the corresponding nuclei in tetramethylsilane. ^{29}Si{^{1}H} heteronuclear correlation (HETCOR) NMR experiments[25−27] were conducted under conditions of magic-angle spinning at 4.0 kHz and consisted of a 9.0 μs ^{1}H 90° pulse, followed by a 3 ms contact time for cross-polarization. High-power proton decoupling, with an effective spin-locking frequency $\nu_1 = 35$ kHz, was applied during the detection period to remove broadening effects from ^{1}H−^{29}Si dipolar couplings. Time proportional phase incrementation (TPPI) was used for phase sensitivity.[28] ^{13}C{^{1}H} HETCOR/WISE NMR experiments[28,29] were conducted under conditions of MAS at 3 kHz and consisted of a 7.5 μs ^{1}H 90° pulse, followed by a 1 ms contact time for cross-polarization. Continuous-wave proton decoupling ($\nu_1 = 35$ kHz) was applied during the detection period. For both the ^{29}Si{^{1}H} and ^{13}C{^{1}H} HETCOR spectra, 50 Hz exponential line broadening was applied in the t_2 time domain, followed by real-to-real Fourier transformation of the t_1 domain, as required by TPPI conditions to obtain the final spectrum. Spectral assignment of $EO_{106}-PO_{70}-EO_{106}$ proton NMR peaks was achieved by correlating the ^{1}H NMR signals with known ^{13}C NMR resonances in a liquid-state 2D ^{13}C{^{1}H} HETCOR spectrum of the F127 block copolymer dissolved in 5 wt % solution in ^2H_2O (see Supporting Information).

For the block copolymer/silica monoliths, the different ^{29}Si NMR peaks correspond to species with different numbers of pendant siloxane groups, whose chemical shifts have previously been identified;[30] they are denoted by the standard Q^n notation, where n is the number of Si−O−Si bridges that are associated with a given silicon site.[31] The extents of condensation of the inorganic silica networks, as reflected by the relative fractions of Q^3 and Q^4 silica species (see Table 1), were

Table 1. Synthesis Parameters Used To Prepare $EO_{106}-PO_{70}-EO_{106}$ (F127) Block Copolymer/Silica Composites and Accompanying 1D ^{29}Si MAS NMR and XRD Characterization Results[a]

wt % F127	TEOS:H_2O:HCl:EtOH:F127 (mol)	^{29}Si MAS NMR Q^4:Q^3	XRD d_{100} (±0.4 nm)	mesostructural order
0	1:9:0.006:0.0:0.0	1.0		homogeneous
25	1:9:0.006:2.7:0.0016	0.78		homogeneous
40	1:9:0.006:5.3:0.0032	0.75		homogeneous
50	1:9:0.006:8.0:0.0048	0.62	11.5	poorly ordered aggregates
57	1:9:0.006:10.6:0.0064	0.54	11.2	hexagonal/wormlike
62	1:9:0.006:13.1:0.0079	0.41	12.0	hexagonal

[a] The weight percents of the F127 block copolymer in the final composites are based on the final dried composite, assuming complete condensation of the silica. Higher silica Q^4:Q^3 ratios indicate greater extents of silica polymerization. Mesostructural order was determined from XRD and TEM analyses.[51]

measured by ^{29}Si MAS NMR using single-pulse experiments with a 300 s recycle delay.

Proton $T_{1\rho}$ relaxation times were measured at room temperature by directly observing the proton signals.[32] The pulse sequence employed consisted of a 10.5 μs 90° ^1H pulse, followed by an ^1H spin-locking field of $\nu_1 = 42$ kHz of variable duration. Typically, the spin-locking field was applied for 0.010−25 ms to sample the expected range of relaxation times. Spin diffusion did not appear to average the proton relaxation behaviors, as the "fast" and "slow" PEO and PPO moieties appeared to be sufficiently separated to contribute proton NMR signals with distinct relaxation rates.

Results and Discussion

Characterization of transparent block copolymer/silica monoliths (Figure 1) prepared using amphiphilic $EO_{106}-PO_{70}-EO_{106}$ (F127) block copolymer species reveals that the degree of mesostructural ordering in the final composite depends strongly upon the concentration of the block copolymer. Above a threshold of ca. 50 wt % F127 block copolymer, TEM, XRD, and NMR measurements provide evidence of mesostructural ordering, which increases with the block copolymer concentration in the materials.

Mesoscopic Ordering from TEM and X-ray Diffraction. For the transparent $EO_{106}-PO_{70}-EO_{106}/SiO_2$ monoliths prepared with block copolymer concentrations greater than ca. 50 wt %, TEM images reveal appreciable mesoscopic structural order. For example, the TEM images in Figure 2a,b show well-organized hexagonal mesostructures in the 62 wt % copolymer sample (the same as shown in Figure 1). Figure 2a shows a TEM image of a highly ordered hexagonal array of aggregates, viewed perpendicular to the (0001) hexagonal plane. Figure 2b shows the hexagonal arrays viewed from the side, revealing uniform periodicity that persists over large domain sizes (>1 μm^2), which are observed throughout the majority of the sample.

Similar mesostructural features are observed in Figure 3 for a transparent block copolymer/silica monolith prepared with 57 wt % F127. However, the lower concentration of structure-directing block copolymer species leads to a lower overall degree of mesoscopic order. Figure 3a shows a TEM image of a region of hexagonally packed cylinders with relatively uniform ordering, though with some modulation of aggregate features visible. In other regions within the same sample, less-ordered wormlike aggregates are also observed, as shown in Figure 3b. Further reduction of the block copolymer concentration to 50 wt % produced a transparent composite with a mesostructure composed exclusively of poorly ordered wormlike aggregates (Figure 4); no hexagonal mesostructural features were observed by TEM. Samples possessing 25 and 40 wt % $EO_{106}-PO_{70}-EO_{106}$ displayed no discernible mesoscopic features of any kind in the TEM images (not shown here).

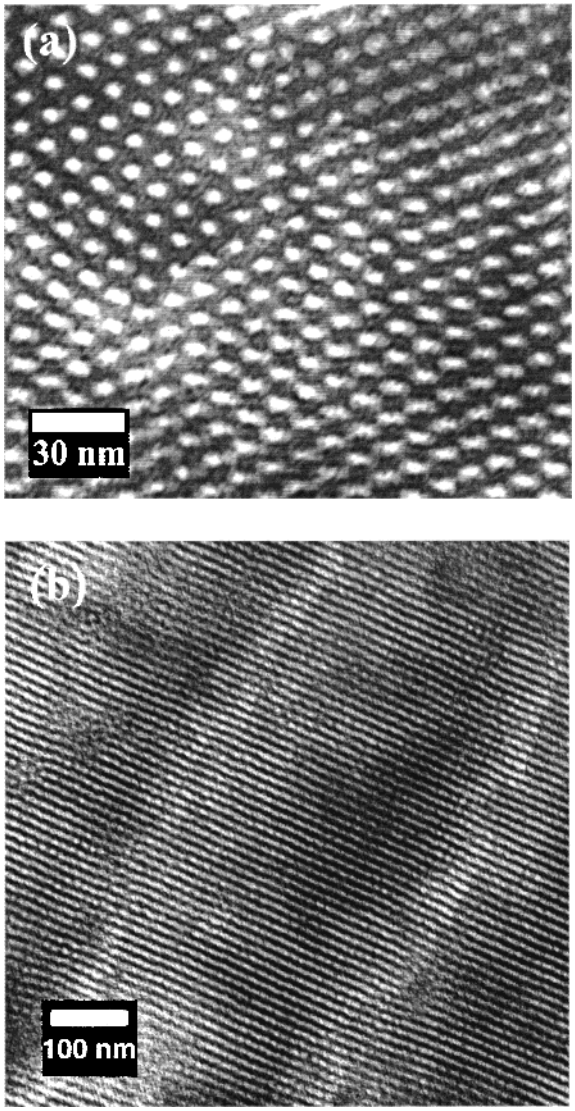

Figure 2. Representative TEM micrographs of the 62 wt % $EO_{106}-PO_{70}-EO_{106}/SiO_2$ transparent composite shown in Figure 1 revealing (a) a well-ordered hexagonal array of cylindrical aggregates viewed end-on and (b) hexagonal arrays of aggregates viewed from the side. Regions in the sample that are predominantly organic appear light, in contrast to the darker silica. Note the scale bars are different for the two images.

X-ray diffraction results confirm that mesostructural ordering of the $EO_{106}-PO_{70}-EO_{106}/SiO_2$ composites increases with the concentration of F127 block copolymer. Typical powder X-ray diffraction patterns are shown in Figure 5 for the composites shown in Figures 2−4 and listed in Table 1. As the concentration of $EO_{106}-PO_{70}-EO_{106}$ F127 was increased from 25 to 62

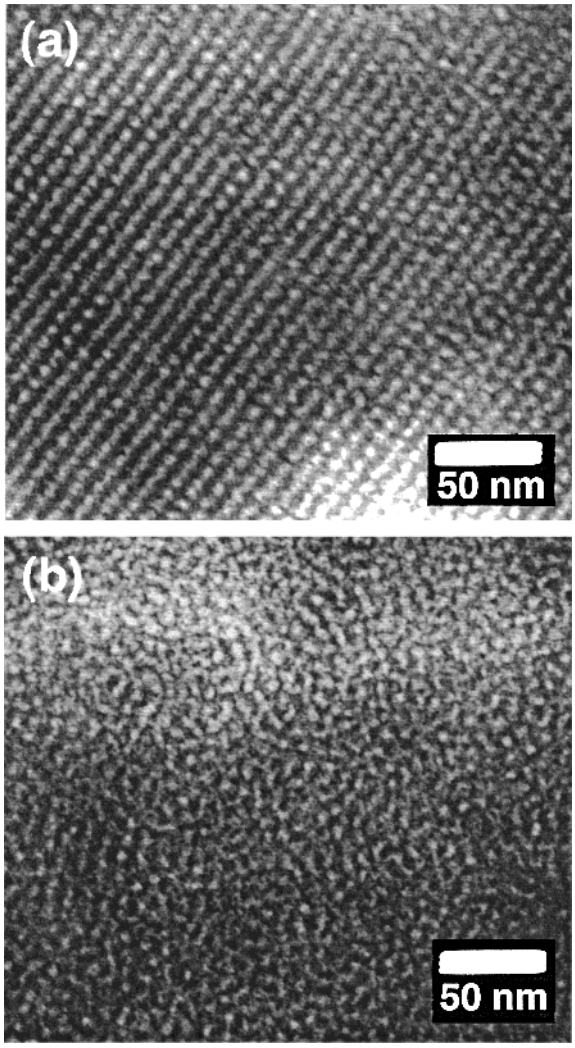

Figure 3. TEM micrographs of a 57 wt % $EO_{106}-PO_{70}-EO_{106}/SiO_2$ transparent composite; different regions of the monolith display predominantly (a) modulated hexagonally packed cylinders (viewed from the side) or (b) wormlike aggregates. In this sample, hexagonal domain sizes were typically <0.5 μm^2, while the wormlike domains were relatively large (>1 μm^2).

wt %, a low-angle reflection with a d spacing of 11−12 nm appeared and intensified above 40 wt % block copolymer, below which no discernible X-ray scattering peaks were observed. For materials containing 50, 57, or 62 wt % of the block copolymer species, the materials yielded powder XRD patterns with d_{100} peaks at 11.5, 11.2, and 12.0 nm, respectively. The peaks became more narrow and intense as the block copolymer concentration was increased over this range of compositions and conditions, reflecting increased long-range mesostructural ordering in these materials. For the 62 wt % sample, a broad higher order reflection near $q = 1.1$ nm^{-1} is present that cannot be conclusively assigned to a particular mesophase. Low or absent signal intensities from higher order reflections are consistent with the TEM images in Figure 2, which show relatively rough or diffuse interfaces between the silica and hydrophobic copolymer regions.[33] Whereas strongly cooperative silica−surfactant assembly mechanisms enhance such ordering in alkaline in MCM-type syntheses,[4] the silica appears to disrupt the mesophase organization of the concentrated block copolymer species under the acidic conditions examined.

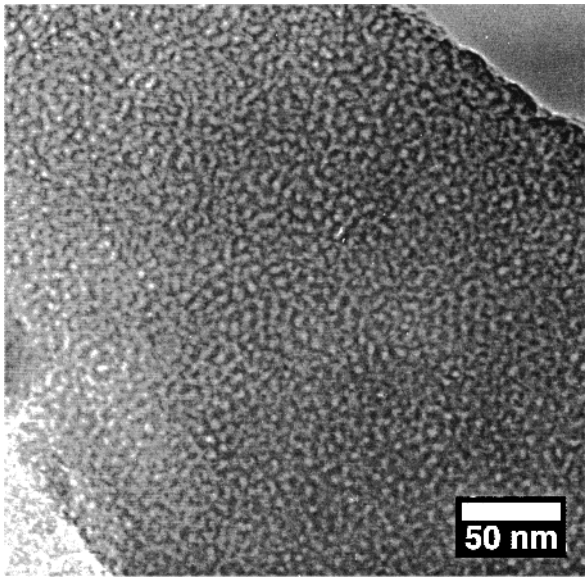

Figure 4. TEM image of a 50 wt % $EO_{106}-PO_{70}-EO_{106}/SiO_2$ transparent composite showing poorly ordered aggregates of the block copolymer (light) within the silica matrix (dark). These structures persisted over the entire sample.

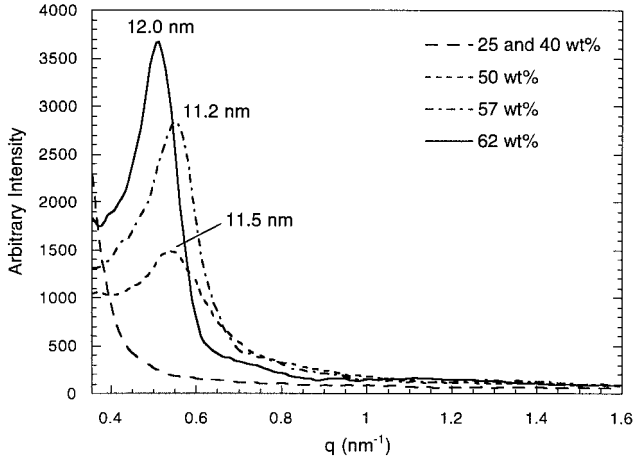

Figure 5. Small-angle powder X-ray diffraction patterns of $EO_{106}-PO_{70}-EO_{106}/SiO_2$ transparent monoliths containing different concentrations of block copolymer (see Table 1). Samples were prepared by gentle grinding of the monoliths to form powders (as for the TEM images in Figures 2−4); equivalent volumes were used for each XRD measurement. Peak widths (fwhm) for the dominant reflections were measured to be 0.30, 0.18, and 0.13 nm^{-1} for the 50, 57, and 62 wt % F127 composites, respectively.

It was not possible from the analyses of ground powder samples performed to determine the orientation of the hexagonal phases. However, preliminary results of 2D X-ray diffraction analyses of monolithic pieces show the hexagonal cylinders tend to orient parallel to the bottom of the sample vial and form large domains.[34]

Solid-State NMR: Block Copolymer Species Aggregation and Distribution. While the mesoscopic morphologies of the monoliths can be established through XRD and TEM analyses, the molecular interactions that form the basis of the self-assembled structures may be examined by powerful two-dimensional (2D) solid-state NMR methods and NMR relaxation analyses. Solid-state 2D ^1H, ^2H, ^{13}C, and ^{29}Si NMR measurements have been widely used to characterize the molecular environments and dynamics of polymeric species in situ.[28] In

addition, solid-state ^{1}H and ^{29}Si NMR experiments have been used to examine the molecular structures[25,30,35] and silanol contents of silica and organically modified silica hybrid materials.[26,36]

In the present study, a combination of ^{1}H, ^{13}C, and ^{29}Si NMR methods have been adapted to investigate the aggregation and local distributions of the F127 block copolymer segments within the composite samples. This is achieved by correlating ^{1}H, ^{13}C, and ^{29}Si chemical shifts, mediated by heteronuclear dipole−dipole couplings between nuclei in the different block copolymer moieties and the silica framework. Such couplings depend strongly on the respective mobilities and separations of the nuclei involved, which allow local structural and dynamical properties of the copolymer blocks to be examined, including their proximity to the silica framework. Such measurements can be analyzed to determine the degree of microphase separation of the copolymer blocks within the material. For example, under ambient conditions, block segments that are intimately mixed or in interfacial contact with the rigid silica network are expected to have considerably lower mobilities than block segments that are microphase-separated in molecular environments similar to the neat copolymer. These different dynamical properties can be readily distinguished by the strengths of the ^{1}H−^{29}Si and ^{1}H−^{13}C dipolar couplings and by ^{1}H NMR relaxation rates.

In particular, molecular proximities and molecular interface structures can be assessed by using heteronuclear chemical shift correlation (HETCOR) NMR spectroscopy. The same NMR pulse sequence has also been used to resolve the dynamic properties of different molecular species, in an otherwise identical experiment known as the wide-line separation experiment (WISE).[29] The HETCOR/WISE experiments have been described in detail by Vega for ^{1}H−^{29}Si correlation studies of silanol groups in silicas and zeolites[25] and by Schmidt-Rohr et al. for ^{1}H−^{13}C correlations in heterogeneous polymer blends.[29] This technique yields increased resolution of ^{1}H and ^{13}C or ^{29}Si peaks by correlating specific chemical shifts in a two-dimensional (2D) spectrum that allows dipole−dipole-coupled nuclei to be identified.[28,37] This is achieved by creating ^{1}H magnetization, which can be transferred during the mixing time of the 2D experiment to nearby ^{13}C or ^{29}Si nuclei via heteronuclear dipole−dipole couplings. Due to the strong homonuclear ^{1}H−^{1}H dipole couplings present, magnetization can also be transferred between neighboring ^{1}H nuclei via spin diffusion before cross-polarizing to ^{13}C or ^{29}Si nuclei. The length scale probed depends on the magnitude of the heteronuclear and typically strong homonuclear ^{1}H−^{1}H couplings; the latter can efficiently distribute ^{1}H magnetization among protonated moieties during the mixing time. Under the experimental conditions used here, such ^{1}H spin diffusion during the mixing time is expected to lead to intensity correlations between ^{1}H and either ^{13}C or ^{29}Si nuclei that are separated by ∼1.1 nm or less.[38] The HETCOR experiment is capable of providing detailed structural information regarding molecular and interfacial environments in close proximity to the various protonated block copolymer moieties, namely the PEO and PPO block copolymer backbones and pendant methyl groups on the PPO segments.

^{13}C{^{1}H} WISE NMR: Copolymer Segment Mobilities. Proton NMR peak assignments for the different protonated moieties of the block copolymer were established from the liquid-state 2D ^{13}C{^{1}H} HETCOR spectrum (see Supporting Information) of the F127 block copolymer dissolved in aqueous solution. This permitted subsequent identification of ^{1}H−^{13}C or ^{1}H−^{29}Si intensity correlations in the solid-state HETCOR spectra involving specific moieties in the PEO−PPO−PEO/silica composites.

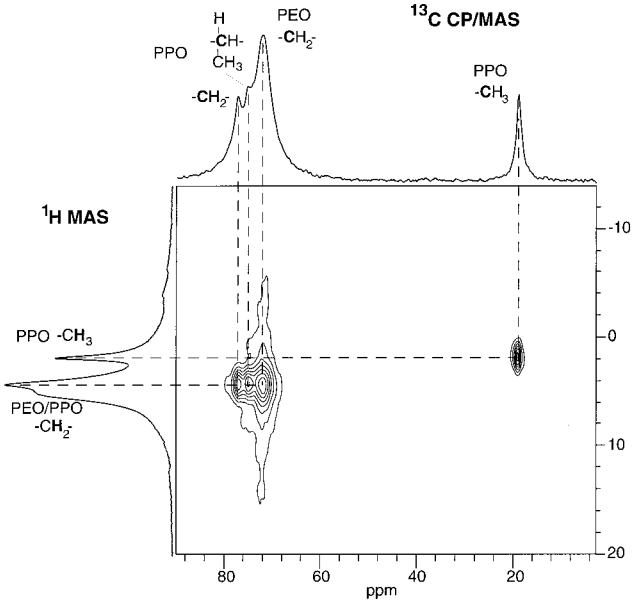

Figure 6. Room-temperature 2D ^{13}C{^{1}H} WISE NMR spectrum of the 50 wt % EO_{106}−PO_{70}−EO_{106}/SiO_2 composite from Figure 4. Separate ^{13}C and ^{1}H MAS spectra are plotted along their respective axes. The different line widths observed in the 2D contour plot result from different mobilities of the PEO and PPO moieties: the narrower ^{13}C line widths associated with the PPO backbone carbon atoms reflect significantly higher mobilities of the PPO species compared to the PEO segments, consistent with partial microphase separation of the PPO species away from the rigid silica matrix.

To the extent that microphase separation of the PEO−PPO−PEO/silica systems has occurred, mobility and internuclear separation differences will be reflected in the ^{13}C{^{1}H} WISE line shapes observed for the different block copolymer components. In general, the line width of a homogeneously broadened signal is larger for rigid samples than for materials with high degrees of molecular motion, which tends to average the dipole−dipole interactions and produce a narrower peak. Figure 6 shows a 2D ^{13}C{^{1}H} WISE spectrum for the 50 wt % EO_{106}−PO_{70}-EO_{106}/SiO_2 composite, with separately acquired 1D ^{13}C CP-MAS and ^{1}H MAS spectra plotted along the respective axes. Though several of the ^{1}H peaks are not resolved in the 1D ^{1}H MAS spectrum, they are separated according to the chemical shifts of the ^{13}C species to which they are bonded in the solid-state 2D ^{13}C{^{1}H} WISE spectrum. The relatively narrow (∼1.0 kHz) ^{1}H peak associated with the PPO methyl group (corresponding to a ^{13}C shift of 17 ppm) reflects the relatively high mobility of the $-CH_3$ species. Similar line widths (∼1.5 kHz) are observed in the ^{1}H dimension for the two PPO peaks, located at ^{13}C shifts of 74 and 76 ppm, associated with the PPO backbone carbon moieties. In contrast, the ^{1}H peaks from the PEO backbone protons are broader, with a ^{1}H MAS line width of ∼2.5 kHz that is resolved in the ^{13}C dimension at 72 ppm. Compared to the narrower PPO ^{1}H signals, the broader $-OCH_2CH_2-$ ^{1}H peak indicates that the PEO segments

are less mobile. This is consistent with the greater hydrophilicity of the ethylene oxide blocks and correspondingly stronger PEO interactions with the silica network relative to the PPO blocks.

The ^{1}H MAS line widths measured both for the PEO and PPO blocks in the silica composites are larger than for the corresponding signals in neat $EO_{106}-PO_{70}-EO_{106}$ (∼160 and 70 Hz, respectively), reflecting the influence of the rigid silica framework. When the block copolymer concentration is increased to 57 and 62 wt % F127, equivalent ^{1}H MAS line widths of ∼1.0 kHz are observed (not shown here) for both the PPO and PEO ^{1}H NMR signals. Such similar and relatively narrow line widths indicate that the polymer segments in these microphase-separated systems experience similarly mobile environments. The relatively high molecular mobilities are consistent with reduced interfacial contact between the PEO and PPO blocks and the rigid silica matrix, as the degree of microphase separation and mesoscopic ordering in the composites increases.

For samples in which microphase separation does not occur, occlusion of the block copolymer within the silica matrix can impart significantly greater rigidity to the polymer segments, producing broad ^{1}H lines that become difficult to identify in MAS or 2D WISE spectra. Composites with 25 or 40 wt % $EO_{106}-PO_{70}-EO_{106}$ each produced a 2D ^{13}C{^{1}H} WISE spectrum with an extremely broad, ∼10 kHz wide ^{1}H peak that could not be resolved into its PEO and PPO components. These results indicate that both copolymer blocks in the 25 and 40 wt % F127 samples have low mobilities. This is consistent with XRD (Figure 5) and TEM measurements discussed earlier, which show these composites to be non-mesostructured blends, with the block copolymer species occluded essentially homogeneously within the silica network.

^{29}Si{^{1}H} HETCOR NMR: Silica−Organic Interfacial Interactions. Further evidence for microphase separation of the PEO and PPO copolymer blocks can be found from the spatial distribution of the copolymer segments relative to the silica matrix, as measured from 2D ^{29}Si{^{1}H} HETCOR experiments. Analogous to the ^{13}C{^{1}H} WISE measurements, the ^{1}H−^{29}Si polarization transfer is effective over ∼1 nm distances due to ^{1}H spin diffusion, influenced also by the molecular mobilities of the copolymer segments. Correlated peak intensities between ^{1}H and ^{29}Si resonances in a 2D ^{29}Si{^{1}H} HETCOR spectrum, such as shown in Figure 7, indicate close spatial proximities of the dipole−dipole coupled ^{1}H and ^{29}Si species. The peaks at ca. −90, −100, and −110 ppm in the 1D ^{29}Si MAS spectra shown along the horizontal axes of Figure 7 have been previously assigned to Q^2, Q^3, and Q^4 ^{29}Si species.[30] Peaks in the ^{1}H MAS spectra along the vertical axes in Figure 7 have been identified on the basis of the liquid-state ^{13}C{^{1}H} HETCOR spectrum of the F127 block copolymer, which has been included as Supporting Information.

The ^{29}Si{^{1}H} HETCOR spectra of the $EO_{106}-PO_{70}-EO_{106}/SiO_2$ composites provide molecular-level evidence for increasing microphase separation of the PEO and PPO segments with increasing block copolymer concentrations. The 2D ^{29}Si{^{1}H} HETCOR spectrum in Figure 7a of the 50 wt % block copolymer/silica composite has two peaks corresponding to correlations involving both the PEO and PPO protons and ^{29}Si species. In particular, resolved peaks are observed that reflect magnetization transfer to Q^3 ^{29}Si species (−102 ppm) from the $-OCH_2-$ protons (4.0 ppm, attributed to both the PEO and PPO backbones) or from the PPO methyl group protons (1.2 ppm). A one-dimensional ^{1}H MAS slice taken through the Q^3 ^{29}Si peak is plotted on the right side of Figure 7a, which clearly displays these resolved proton correlations. The pronounced shoulder on the low-field side of the $-OCH_2-$ ^{1}H peak (∼4.5 ppm) is due to the presence of Si−OH silanols associated with some Q^3 groups, which do not interfere with the analysis. Weaker correlations are also observed between Q^2 and Q^4 ^{29}Si species and the PEO and PPO backbone moieties. The existence of correlations involving protons from both the PEO and PPO blocks and ^{29}Si species in the silica network demonstrates that both copolymer blocks are in close proximity (∼1 nm) to the silica matrix. These results corroborate the TEM, XRD, and ^{13}C{^{1}H} WISE measurements in Figures 4, 5, and 7, which indicate that microphase separation of the copolymer blocks is incomplete at concentrations of 50 wt % F127 and below. The ^{13}C{^{1}H} WISE and ^{29}Si{^{1}H} HETCOR spectra for the 50 wt % block copolymer/silica composite establish that the PEO blocks interact with, and perhaps penetrate into, the silica network.

^{29}Si{^{1}H} HETCOR spectra of composites containing concentrations of PEO−PPO−PEO block copolymer above 50 wt % reveal increased degrees of microphase separation between the two copolymer blocks and the silica network. The 2D ^{29}Si{^{1}H} HETCOR spectrum in Figure 7b of the 62 wt % $EO_{106}-PO_{70}-EO_{106}$/silica composite reveals two distinct peaks that correlate signal intensity from the $-OCH_2CH_2-$ PEO backbone protons at 4.0 ppm with that from Q^2 and Q^3 ^{29}Si species at −92 and −102 ppm, respectively. This confirms the close proximity of the PEO segments and the silica network. However, no correlated intensity is observed between the ^{29}Si Q^3 species and protons of the PPO $-CH_3$ group, in contrast to the ^{29}Si{^{1}H} HETCOR spectrum (Figure 7a) for the 50 wt % composite. The one-dimensional ^{1}H MAS slice taken through the Q^3 peak plotted in Figure 7b shows evidence for a single correlation between the backbone protons to the Q^3 ^{29}Si. The lack of intensity correlations between the ^{1}H peak(s) associated with the PPO blocks and the ^{29}Si species in the silica framework demonstrates that the majority of PPO species have microphase-separated to distances greater than ca. 1 nm from the silica matrix. Such molecular evidence for microphase separation in this sample is in agreement with the ordered hexagonal mesophase observed by TEM (Figure 2) and XRD (Figure 5). These results are consistent with the formation of block copolymer aggregates composed of central PPO cores surrounded by annular shells or layers of PEO ∼1.1 nm thick that interact strongly with the silica network.[38] The schematic diagrams in Figure 7 depict the relative partitioning and mesostructural ordering of the copolymer blocks and silica that are consistent with the NMR, XRD, and TEM results for the respective samples.

^{1}H NMR Relaxation Analyses: Extents of Microphase Separation. The dynamic behaviors of the different copolymer blocks can be used to assess their respective degrees of interaction with the silica matrix, in particular, when microphase separation of the PEO and PPO blocks may not be complete. In such cases, the relative fractions of microphase-separated PEO and PPO segments can be estimated from analyses of ^{1}H NMR relaxation rates, which can distinguish and

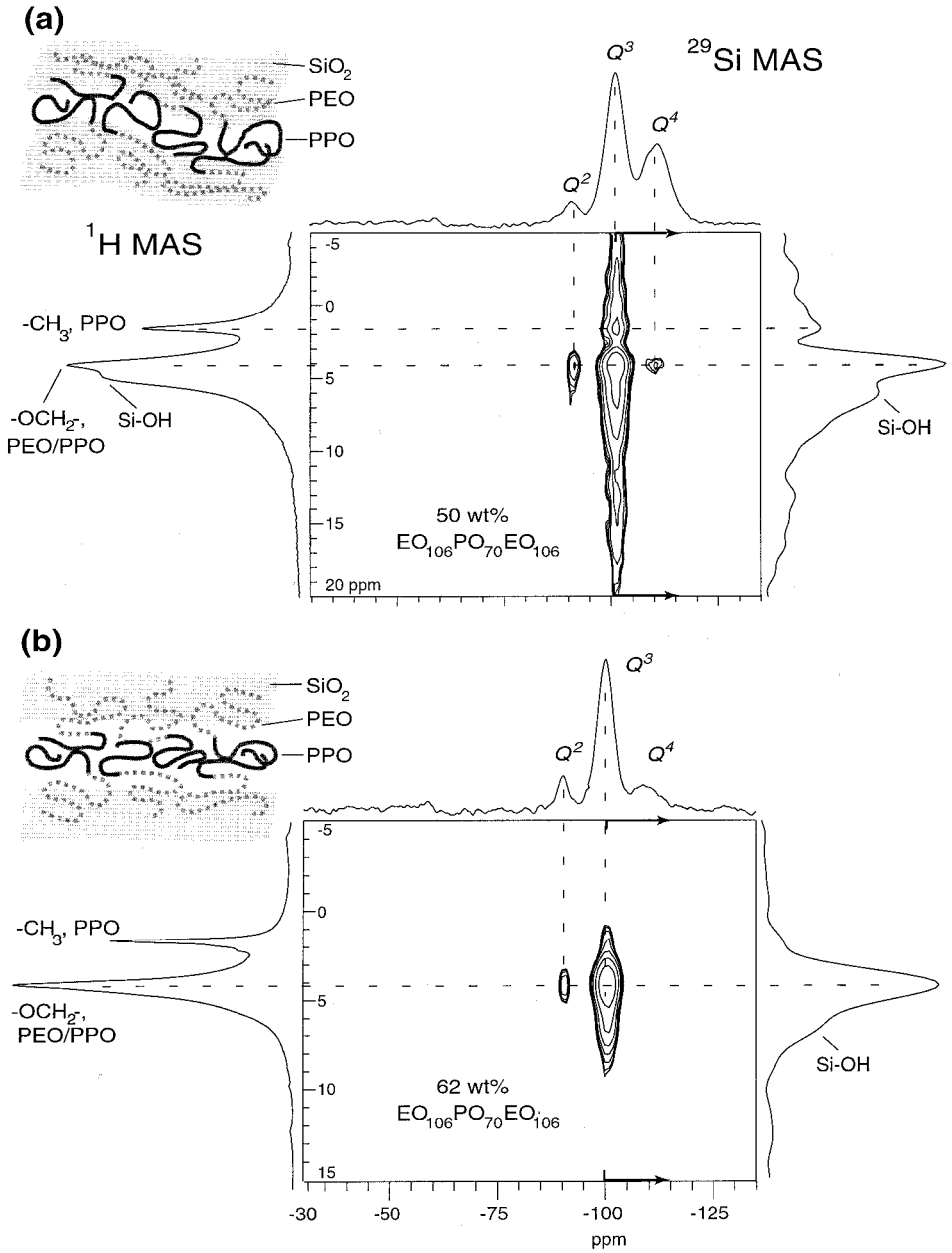

Figure 7. Room-temperature 2D ^{29}Si{^{1}H} HETCOR NMR spectra for the (a) 50 wt % and (b) 62 wt % $EO_{106}-PO_{70}-EO_{106}/SiO_2$ composites. Separate ^{29}Si MAS and ^{1}H MAS spectra are plotted along their respective axes. Short 3 ms contact times were used to probe molecularly proximate species (separation distances < 1 nm). In (a), strong correlated intensity is observed between proton signal(s) from the $-OCH_2-$ PEO/PPO backbone and ^{29}Si signals from Q^3 ^{29}Si species; in addition, a weaker but significant intensity correlation is evident between the PPO $-CH_3$ protons and the Q^3 silica. In (b), no such correlated intensity is observed between the PPO methyl protons and any of the silica species, while strong intensity correlations are evident between $-OCH_2-$ protons (attributed to the PEO backbone) and both Q^3 and Q^2 ^{29}Si species. One-dimensional slices through the Q^3 plane have been plotted on the right side of the spectra to demonstrate correlated intensities more clearly. Schematic diagrams accompanying the spectra depict the local and mesoscopic structures of the composites consistent with the NMR, XRD, and TEM data.

quantify block copolymer moieties in "mobile" and "rigid" environments.

A variety of NMR relaxation measurements have been used previously to examine polymer dynamics,[39−41] degrees of crystallinity in neat polymer systems,[42] and microphase separation in polymer blends.[43,44] As in semicrystalline polymer systems, the PEO and PPO blocks within the F127-silica composites are expected to exhibit molecular mobilities in two regimes: "fast" segments with relatively high mobilities in microphase-separated polymer aggregates and "slow" segments with significantly reduced mobilities resulting from occlusion or interfacial interactions with the rigid silica matrix. Such moieties and their mobilities may be distinguished and analyzed on the basis of a series of ^{1}H NMR spectra, parametrized to extract spin−lattice relaxation times in the rotating frame ($T_{1\rho}$) for species with resolved ^{1}H peaks.[32] The relaxation time $T_{1\rho}$ is a characteristic time constant that is a measure of the rate at which an ensemble of excited nuclear spins returns to thermal equilibrium under an applied magnetic field with respect to the rotating frame of reference. The rates at which ^{1}H spins relax depend on the dipolar coupling strengths between the protons and the "lattice", which are strong functions of species mobility. For the block copolymer/silica composites under investigation, copoly-

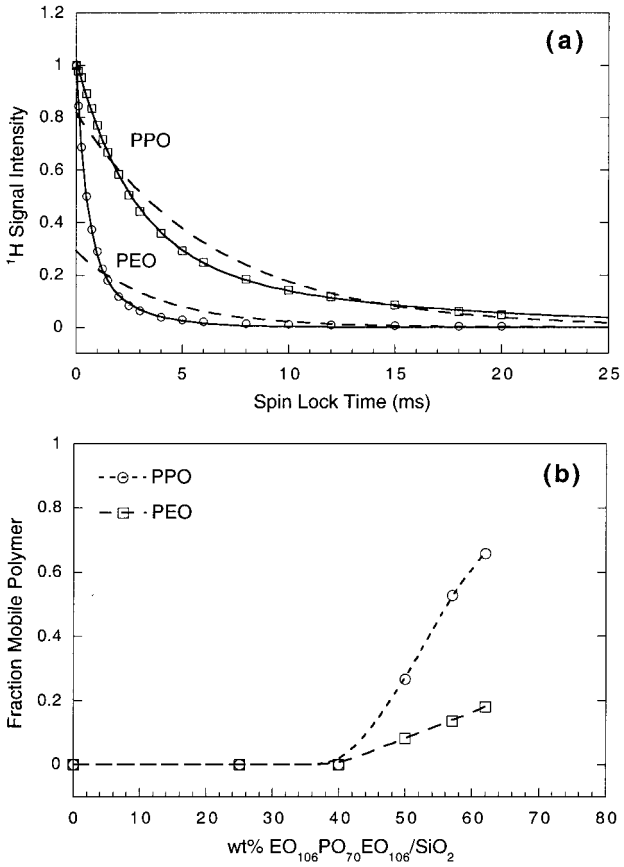

Figure 8. ^{1}H $T_{1\rho}$ NMR relaxation time measurements at room temperature obtained for the $EO_{106}-PO_{70}-EO_{106}/SiO_2$ composites containing different concentrations of block copolymer. (a) A representative plot (here, for the 57 wt % block copolymer sample) of the ^{1}H signal intensities measured for the $-OCH_2-$ (predominantly PEO) and $-CH_3$ (PPO) moieties as a function of spin-lock duration. $T_{1\rho}$ relaxation constants for the "fast" and "slow" fractions of the PEO and PPO segments are calculated from biexponential fits to the data ($\chi^2 < 0.0002$ in all cases), represented by the solid lines. The dotted lines show the inadequacy of monoexponential fits. (b) Summarized results showing the fractions of "fast" PEO and PPO segments, based on the biexponential fits to $T_{1\rho}$ data, such as those calculated in (a). The fractions of "fast" PEO and PPO species increase with increasing concentration of block copolymer in the composite, consistent with increasing microphase separation. The lines through the data points have been added to guide the eye.

mer segments that interact strongly with the silica matrix will experience reduced molecular mobilities and thus have shorter $T_{1\rho}$ relaxation times, compared to more mobile segments in microphase-separated regions, which will be characterized by longer $T_{1\rho}$ values.

Proton $T_{1\rho}$ values were measured using standard techniques[32] to acquire a series of 1D ^{1}H MAS NMR spectra obtained using a spin-lock field of systematically varied duration. Under such conditions, proton signal intensity decays due to mobility-dependent dipolar interactions. The intensity of each resolved ^{1}H peak in the resulting 1D ^{1}H MAS spectra was recorded as a function of spin-lock time to produce a relaxation-induced decay curve for each peak. A representative ^{1}H MAS signal intensity curve is shown in Figure 8a for the 57 wt % $EO_{106}-PO_{70}-EO_{106}/SiO_2$ composite. Typically, the decay of ^{1}H peak intensity is modeled as an exponential function to determine the characteristic time constant $T_{1\rho}$ of the mobility-induced relaxation process(es). However, if a peak contains signal contributions from components with different motional characters, a multiexponential model can be used to obtain an improved fit to the signal decay curve, from which multiple time constants are then extracted.[42] These models are usually expressed as a sum of exponentials, e.g., $A_1e^{-t/T_{1\rho,1}} + A_2e^{-t/T_{1\rho,2}}$, where the relative amplitudes of the different exponential terms can be used to estimate the fraction of species in the mobility regimes that are characterized by relaxation times $T_{1\rho,1}$ and $T_{1\rho,2}$. In general, such $T_{1\rho}$ analyses will not be unique.

In combination, however, with the molecular and mesostructural insights provided by the 2D HETCOR/WISE, XRD, and TEM measurements discussed above, the use of biexponential $T_{1\rho}$ analyses to characterize "fast" and "slow" block copolymer segments in microphase-separated PEO−PPO−PEO/SiO_2 composites is reasonable. Furthermore, while the $T_{1\rho}$ values alone are not unique to the molecular motions or processes, it is nevertheless possible to estimate the relative populations of moieties with significantly different types of intrinsic dynamics.[45] Figure 8a shows ^{1}H MAS signal intensities plotted as functions of spin-lock time for the PEO and PPO blocks in the 57 wt % block copolymer/silica composite; the ^{1}H signals measured were the $-CH_3$ PPO peak at 1.0 ppm and the $-OCH_2-$ PEO/PPO peak at 3.5 ppm.[46] Biexponential models (Figure 8a, solid lines) fit the $T_{1\rho}$ data quite well for both the PEO and PPO segments, with goodness of fit parameters better than $\chi^2 < 0.0002$ in all cases. Separate monoexponential fits to the PEO and PPO ^{1}H decay curves (Figure 8a, dotted lines) do not provide good representations of the data, validating the need for multiexponential analysis. Quantitative estimates of the fast and slow fractions of the PEO and PPO copolymer blocks were calculated from the relative amplitudes of the two fitted exponentials characterized by long and short $T_{1\rho}$ values, corresponding to "fast" and "slow" polymer moieties, respectively, as summarized in Table 2.

For both the PEO and PPO polymer blocks, the overall fractions displaying "fast" character increase with the concentration of the structure-directing block copolymer species, as evident from both the ^{1}H $T_{1\rho}$ and line width measurements summarized in Table 2 and Figure 8b. At 25 and 40 wt % block copolymer, the broad (>2 kHz) ^{1}H MAS peaks associated with the PEO and PPO species decay rapidly, yielding $T_{1\rho}$ values between 0.11 and 1.17 ms that indicate "slow" polymer environments. The $T_{1\rho}$ values of the PEO and PPO segments in the composite are both short, relative to those of their fast counterparts in the neat F127 copolymer ($T_{1\rho} = 32$ and 25 ms, respectively) under otherwise identical conditions, most likely due to interactions with the silica matrix. These results are consistent with the majority of the PEO and PPO species being distributed essentially homogeneously (within ~9 Å, limited by spin diffusion) within the silica composite blends. Whereas binary systems containing 25 or 40 wt % $EO_{106}-PO_{70}-EO_{106}$ in water are anticipated to form micellar or cubic aggregates,[47,48] mesostructural order in composites with these concentrations is apparently disrupted by the presence of the silica. This is in accord with the absence of XRD peaks (Figure 5) and the absence of aggregates in TEM images (not shown here) for these materials. Collectively, these results confirm the absence of mesophase ordering in the $EO_{106}-PO_{70}-EO_{106}/SiO_2$ composites prepared with 40 wt % or lower concentrations of F127 block copolymer.

Table 2. Summary of Results from ^{1}H $T_{1\rho}$ and NMR Line-Shape Analyses for F127−Silica Composites Containing Different Concentrations of the Block Copolymer[a]

	PEO				PPO			
wt % F127	fraction "fast" segments	"fast" $T_{1\rho}$ (ms)	"slow" $T_{1\rho}$ (ms)	^{1}H MAS line width (Hz)	fraction "fast" segments	"fast" $T_{1\rho}$ (ms)	"slow" $T_{1\rho}$ (ms)	^{1}H MAS line width (Hz)
25	0		0.11 ± 0.01	∼3500	0		0.11 ± 0.01	∼3500
40	0		0.56 ± 0.01	∼2200	0		1.17 ± 0.04	∼2200
50	0.08 ± 0.01	2.9 ± 0.2	0.60 ± 0.01	770	0.27 ± 0.03	7.4 ± 0.7	1.49 ± 0.06	284
57	0.14 ± 0.01	4.0 ± 0.3	0.73 ± 0.01	530	0.53 ± 0.02	8.5 ± 0.3	1.52 ± 0.07	142
62	0.17 ± 0.01	12.7 ± 0.6	1.20 ± 0.01	280	0.66 ± 0.04	27 ± 3	3.55 ± 0.04	58
100	0.85 ± 0.02	32.3 ± 0.7	0.16 ± 0.03	160	0.76 ± 0.01	25 ± 1	0.46 ± 0.09	70

[a] Fast component fractions and $T_{1\rho}$ values are from biexponential fits to ^{1}H signal decay curves, such as shown in Figure 8.

At higher concentrations of the block copolymer, increased microphase separation of the blocks leads to higher fractions of "fast" PEO and PPO species, as evidenced by progressively longer ^{1}H $T_{1\rho}$ values and narrower ^{1}H MAS line widths (Figure 8b, Table 2). For example, for the composite containing 50 wt % F127 block copolymer, the PEO and PPO ^{1}H MAS line widths are significantly narrower (770 and 284 Hz, respectively) than those measured for the 40 wt % sample (2200 Hz for both PEO and PPO). The narrower line widths reflect partial separation of the copolymer blocks, particularly the PPO, from the silica. Table 2 shows that, for the 50 wt % F127/SiO_2 composite, 27% of the PPO segments are estimated to be in "fast" environments, characterized by a relatively long $T_{1\rho} = 7.4$ ms, while the remainder experience relatively "slow" environments, with $T_{1\rho} = 1.49$ ms. The ^{1}H $T_{1\rho}$ value of the fast PPO segments (7.4 ms) in the composite is intermediate between that of fast PPO moieties in the neat block copolymer ($T_{1\rho} = 25$ ms) and the slow PPO component in the silica composite ($T_{1\rho} = 1.49$ ms). This suggests that the fast PPO segments in the 50 wt % composite interact with the silica to some degree and thus are not as mobile as in the neat F127 system. By comparison, analysis of the $T_{1\rho}$ data for the PEO moieties indicates that they are predominantly (>90%) slow, with a short $T_{1\rho} = 0.60$ ms. These results are consistent with the ^{29}Si{^{1}H} HETCOR spectrum in Figure 7a, which shows that a significant fraction of the PPO and PEO segments are within close proximity (∼1 nm) to the silica network and the presence of poorly ordered aggregates observed by TEM (Figure 4). In combination, these results establish that the 50 wt % F127−silica composite possesses a poorly ordered mesostructure with partially microphase-separated PPO and a majority of the PPO and PEO segments that are within close proximity to, and are likely occluded in, the silica matrix. Separate ^{1}H NMR spin-diffusion studies support at least partial occlusion of PEO segments within the silica matrix, based on the appearance of a strong cross-polarization signal, even for very short diffusion times (∼0.5 ms).[49] Morphological features that are consistent with all experimental results for the 50 wt % F127−silica composite are shown schematically in Figure 7a.

In $EO_{106}-PO_{70}-EO_{106}/SiO_2$ composites containing 57 and 62 wt % block copolymer, proton $T_{1\rho}$ relaxation analyses and ^{1}H MAS line width measurements (Figure 8, Table 2) indicate high degrees of microphase separation. For these materials, the longer ^{1}H PPO $T_{1\rho}$ relaxation times (8.5 and 27 ms, respectively) and narrower ^{1}H MAS line widths (142 and 58 Hz) indicate substantially increased mobilities of the PPO blocks, consistent with increased microphase separation and mesostructural order in these materials. The PPO blocks are predominantly "fast", with estimated fast fractions of 0.53 and 0.66 in the two samples, respectively, while the PEO species remain largely "slow", with corresponding slow fractions of 0.86 and 0.83. In particular, the $T_{1\rho}$ value (27 ± 3 ms) measured for the fast PPO fraction in the 62 wt % composite is equivalent to that (25 ± 1 ms) of the amorphous PPO regions in the neat block copolymer, suggesting that the fast PPO segments are unperturbed by the silica matrix. These results corroborate the ^{29}Si{^{1}H} HETCOR measurements (Figure 7b), which established that the PPO segments in the 62 wt % sample are spatially/dynamically separated (>1 nm) from the polymerized silica network.

In contrast, the fast PEO species are measured to have a $T_{1\rho}$ value that is considerably lower (12.7 ms) than for the amorphous PEO regions of the neat F127 block copolymer (32.3 ms), suggesting that the fast PEO segments interact with the silica to some degree. The majority (>80%) of the PEO moieties, however, are slow, characterized by a short 1.20 ms $T_{1\rho}$ value, which indicates that the mobilities of the segments are constrained.

It is likely that such "slow" PEO moieties are strongly interacting with, and are possibly occluded in, the silica network, as opposed to being located within nanocrystalline PEO regions within microphase-separated aggregates. In support of this, longer $T_{1\rho}$ values and narrower ^{1}H line widths are measured for the slow PEO segments at higher block copolymer concentrations, indicating increased molecular mobilities of these "slow" species. This is consistent with the existence of occluded, noncrystalline PEO in a less completely cross-linked, and therefore locally less rigid, silica network. As shown in Table 1, substantially smaller Q^4:Q^3 ^{29}Si ratios are observed at higher block copolymer concentrations. Furthermore, the strong correlated peak intensity between Q^3 ^{29}Si species and PEO protons in the ^{29}Si{^{1}H} HETCOR spectrum (Figure 7b) demonstrates that a large fraction of the PEO segments are closely associated with the SiO_2 framework, as opposed to residing within nanocrystalline domains. Moreover, the ca. 1 ms ^{1}H $T_{1\rho}$ values of the "slow" PEO species deviate significantly from that measured for crystalline PEO samples ($T_{1\rho} \sim 0.1$ ms). In addition, previous work[50] on semicrystalline PEO−poly(butylene oxide) block copolymers indicates that high chain-folding energies are expected to discourage the formation of nanocrystallite with dimensions <10 nm, as would be required in these materials. Further research is underway in our laboratories to determine the effects, if any, of PEO crystallinity on the composite structure.

For the 62 wt % $EO_{106}-PO_{70}-EO_{106}/SiO_2$ composite, the 2D NMR, TEM, XRD, and ^{1}H NMR relaxation measurements confirm a high degree of hexagonal

mesostructural order. The results additionally point to a mesoscopic substructure in which the hydrophobic aggregates possess well-separated PPO cores, whose interactions with the silica matrix are shielded by layers or shells of PEO that are ca. 1 nm thick. Such substructural ordering is similar to results of Hillmyer et al., who observed partitioning of PEO−PEE copolymer blocks induced by polymerization of hydrophilic epoxy species in a wholly organic system.[18] In the present system, the PEO segments appear to experience appreciable interactions with the silica matrix and may penetrate into the matrix, as illustrated schematically in Figure 7b.

Conclusion

By adopting a templating strategy based upon selective swelling of microphase-separated amphiphilic PEO−PPO−PEO triblock copolymer species, a series of monolithic transparent $EO_{106}-PO_{70}-EO_{106}/SiO_2$ composites have been synthesized under acidic conditions. For composites with block copolymer concentrations approaching ca. 60 wt %, large (>micrometers) domains are observed with highly ordered hexagonal mesostructures ($d_{100} \sim 12$ nm). In general, for the conditions used, the degree of mesoscopic order in the silica composites diminishes, but not the transparency, as the block copolymer concentration is reduced. No mesostructural ordering is observed below a threshold concentration of ca. 40 wt % F127 copolymer, corresponding to a nearly homogeneous mixture of the block copolymer species in the silica network; the composite remains transparent. 2D $^{13}C\{^1H\}$ WISE and $^{29}Si\{^1H\}$ HETCOR and ^1H relaxation NMR experiments have elucidated in situ molecular-level dynamic and structural details of the silica/organic interfaces and extents of block copolymer microphase separation for composites containing different concentrations of the block copolymer species. Such detailed assessment of the molecular and mesoscopic structures of these composites is likely to allow more refined and quantitative approaches to the synthesis and processing of tailored mesostructurally ordered inorganic−organic composite materials.

Acknowledgment. The authors thank Dr. D. Zhao and Dr. P. Yang for helpful discussions and BASF for donation of the Pluronic F127 block copolymer. This work was supported in part by the NSF Division of Materials Research through the UCSB Materials Research Laboratory under Award DMR-9632716 (N.A.M.), the U.S. Army Research Office under Grant DAAH04-96-1-0443 (B.F.C.), AFSOR AF/F-49620-96-1-0088 (F.S.B.), and the David and Lucile Packard Foundation. B.F.C. is a Camille and Henry Dreyfus Teacher-Scholar and an Alfred P. Sloan Research Fellow.

Supporting Information Available: ^1H and ^{13}C peak assignments for the PEO−PPO−PEO block copolymer, established on the basis of a high-resolution liquid $^{13}C\{^1H\}$ HETCOR NMR spectrum obtained on a 5 wt % $EO_{106}PO_{70}EO_{106}$ in aqueous solution at 298 K. This material is available free of charge via the Internet at http://pubs.acs.org.

References and Notes

(1) Beck, J. S.; Vartuli, J. C.; Roth, W. J.; Leonowicz, M. E.; Kresge, C. T.; Schmitt, K. D.; Chu, C. T. W.; Olson, D. H.; Sheppard, E. W.; McCullen, S. B.; Higgins, J. B.; Schlenker, J. L. *J. Am. Chem. Soc.* **1992**, *114*, 10834.
(2) Schüth, F. *Curr. Opin. Colloid Interface Sci.* **1998**, *3*, 174.
(3) Zhao, D.; Yang, P.; Huo, Q.; Chmelka, B. F.; Stucky, G. D. *Curr. Opin. Solid State Mater. Sci.* **1998**, *3*, 111.
(4) Firouzi, A.; Kumar, D.; Bull, L. M.; Besier, T.; Sieger, P.; Huo, Q.; Walker, S. A.; Zasadzinski, J. A.; Glinka, C.; Nicol, J.; Margolese, D.; Stucky, G. D.; Chmelka, B. F. *Science* **1995**, *267*, 1138.
(5) Huo, Q.; Margolese, D. I.; Ciesla, U.; Feng, P.; Gier, T. E.; Sieger, P.; Leon, R.; Petroff, P. M.; Schüth, F.; Stucky, G. D. *Nature* **1994**, *368*, 317.
(6) Raman, N.; Anderson, M.; Brinker, C. J. *Chem. Mater.* **1996**, *8*, 1682.
(7) Lu, Y.; Gangull, R.; Drewien, C. A.; Anderson, M. T.; Brinker, C. J.; Gong, W.; Guo, Y.; Soyez, H.; Dunn, B.; Huang, M. H.; Zink, J. I. *Nature* **1997**, *389*, 364.
(8) Ogawa, M.; Igarashi, T.; Kuroda, K. *Bull. Chem. Soc. Jpn.* **1997**, *70*, 2833.
(9) Zhao, D.; Yang, P.; Melosh, N.; Feng, J.; Chmelka, B. F.; Stucky, G. D. *Adv. Mater.* **1998**, *10*, 1380.
(10) Tolbert, S. H.; Firouzi, A.; Stucky, G. D.; Chmelka, B. F. *Science* **1997**, *278*, 264.
(11) Attard, G. S.; Glyde, J. C.; Göltner, C. G. *Nature* **1995**, *378*, 366.
(12) Ryoo, R.; Ko, C. H.; Cho, S. J.; Kim, J. M. *J. Phys. Chem. B* **1997**, *101*, 10610.
(13) Raimondi, M. E.; Maschmeyer, T.; Templer, R. H.; Seddon, J. M. *Chem. Commun.* **1997**, *19*, 1843.
(14) Marlow, F.; McGehee, M. D.; Zhao, D.; Chmelka, B. F.; Stucky, G. D. *Adv. Mater.*, in press.
(15) Templin, M.; Franck, A.; Du Chesne, A.; Leist, H.; Zhang, Y.; Ulrich, R.; Schädler, V.; Wiesner, U. *Science* **1997**, *278*, 1795.
(16) Zhao, D.; Feng, J.; Huo, Q.; Melosh, N.; Fredrickson, G. H.; Chmelka, B. F.; Stucky, G. D. *Science* **1998**, *279*, 548.
(17) Göltner, C. G.; Antonietti, M. *Adv. Mater.* **1997**, *9*, 431.
(18) Hillmyer, M. A.; Lipic, P. M.; Hajduk, D. A.; Almdal, K.; Bates, F. S. *J. Am. Chem. Soc.* **1997**, *119*, 2749.
(19) Yang, P.; Zhao, D.; Chmelka, B. F.; Stucky, G. D. *Chem. Mater.* **1998**, *10*, 2033.
(20) Göltner, C. G.; Henke, S.; Weissenberger, M. C.; Antonietti, M. *Angew. Chem., Int. Ed. Engl.* **1998**, *37*, 613.
(21) Holmqvist, P.; Alexandridis, P.; Lindman, B. *Macromolecules* **1997**, *30*, 6788.
(22) Zhao, D.; Huo, Q.; Feng, J.; Chmelka, B. F.; Stucky, G. D. *J. Am. Chem. Soc.* **1998**, *120*, 6024.
(23) Brinker, C. J.; Scherer, G. W. *Sol−Gel Science*; Academic Press: San Diego, 1990.
(24) Hench, L. L.; West, J. K. *Chem. Rev.* **1990**, *90*, 33.
(25) Vega, A. J. *J. Am. Chem. Soc.* **1988**, *110*, 1049.
(26) Fyfe, C. A.; Zhang, Y.; Aroca, P. *J. Am. Chem. Soc.* **1992**, *114*, 3252.
(27) Janicke, M. T.; Landry, C. C.; Christiansen, S. C.; Kumar, D.; Stucky, G. D.; Chmelka, B. F. *J. Am. Chem. Soc.* **1998**, *120*, 6940.
(28) Schmidt-Rohr, K.; Spiess, H. W. *Multidimensional Solid State NMR and Polymers*; Academic Press: New York, 1994; p 478.
(29) Schmidt-Rohr, K.; Clauss, J.; Spiess, H. W. *Macromolecules* **1992**, *25*, 3273.
(30) Maciel, G. E.; Sindorf, D. W. *J. Am. Chem. Soc.* **1980**, *102*, 7607.
(31) Engelhardt, G.; Michel, D. *High-Resolution Solid-State NMR of Silicates and Zeolites*; Wiley & Sons: New York, 1987.
(32) Komoroski, R. *High-Resolution NMR Spectroscopy of Synthetic Polymers in Bulk*; VCH Publishers: Deerfield Beach, FL, 1986.
(33) Diffuse interfaces produce rounded electron density profiles that require fewer Fourier terms to model, thus reducing the number of higher order peaks observed in the resulting XRD pattern (which can be interpreted as the Fourier transform of the structure.)
(34) Melosh, N. A.; Davidson, P.; Chmelka, B. F., manuscript in preparation.
(35) Sindorf, D. W.; Maciel, G. E. *J. Am. Chem. Soc.* **1983**, *105*, 1487.
(36) Zumbulyadis, N.; O'Reilly, J. M. *Macromolecules* **1991**, *24*, 5294.
(37) Ernst, R. R.; Bodenhausen, G.; Wokaun, A. *Principles of Nuclear Magnetic Resonance in One and Two Dimensions*; Oxford University Press: New York, 1994.
(38) In the hexagonal silica/block copolymer composites, ^1H spin diffusion can be modeled as a homogeneous process occurring within each cylindrical aggregate using the spin-diffusion constant for neat PEO: $D = 4.1 \times 10^{-16}$ m^2/s.[43] The range

over which ^{1}H−heteroatom couplings are effective can then be estimated from Einstein's equation for a two- dimensional geometry ($n = 4$) with the characteristic time established by the mixing time (3 ms) used in the 2D HETCOR experiment: $\langle r \rangle = 0.5(nDt_m)^{1/2} \sim 1.1$ nm.
(39) Cheng, J.; Fone, M.; Ellsworth, M. W. *Solid State NMR* **1996**, *7*, 135.
(40) Gentzler, M.; Reimer, J. A. *Macromolecules* **1997**, *30*, 8365.
(41) Zeigler, R. C.; Maciel, G. E. *J. Phys. Chem.* **1991**, *95*, 7345.
(42) Johansson, A.; Tegenfeldt, J. *Macromolecules* **1992**, *25*, 4712.
(43) Schantz, S. *Macromolecules* **1997**, *30*, 1419.
(44) Stejskal, E. O.; Schaefer, J.; Sefcik, M. D.; McKay, R. A. *Macromolecules* **1981**, *14*, 4, 275.
(45) Geppi, M.; Harris, R. K.; Kenwright, A. M.; Say, B. J. *Solid State NMR* **1998**, *12*, 15.
(46) In analyzing the mobilities of the PEO segments, the relative contributions of the PPO and PEO backbone protons to the ^{1}H peak at 3.5 ppm were estimated from the stoichiometric number of −OC**H** protons in the copolymer blocks. The PPO protons were determined to be "fast" or "slow" on the basis of the behavior of the PPO methyl group, whose ^{1}H MAS peak was well resolved. Direct comparison of the PEO and PPO dynamics is not possible on the basis of the $T_{1\rho}$ measurements, because the PEO and PPO relaxation rates were measured from ^{1}H peaks arising from different chemical species (e.g., the $-OCH_2CH_2-$ vs $-CH_3$ moieties).
(47) Alexandridis, P.; Hatton, T. A. *Colloids Surf. A* **1995**, *96*, 1.
(48) Wanka, G.; Hoffmann, H.; Ulbricht, W. *Macromolecules* **1994**, *27*, 4145.
(49) Melosh, N. A. Ph.D. dissertation, in preparation.
(50) Ryan, A. J.; Fairclough, J. P. A.; Hamley, I. W.; Mai, S.; Booth, C. *Macromolecules* **1997**, *30*, 1723.
(51) The notation Q^n denotes the number n of next-nearest-neighbor silica atoms that are bonded via bridging oxygen atoms to a given ^{29}Si site; the ratio Q^4:Q^3 reflects the extent of silica cross-linking, as measured from the relative integrated peak areas in resolved ^{29}Si MAS NMR spectra.

MA9817323